Analysis of the growth process of gold nanorods with time-resolved observation

Yoshiko Takenaka[*]

Venture Business Laboratory, Kyoto University, Kyoto 606-8501, Japan

Hiroyuki Kitahata

Department of Physics, Graduate School of Science, Chiba University, Chiba 263-8522, Japan

(Received 5 March 2009; revised manuscript received 28 May 2009; published 7 August 2009)

Gold nanorods are generated spontaneously in a surfactant solution. We developed an experimental setup where the growth of gold nanorods can be completely stopped at any instant. With this method, a time series of the growth process of gold nanorods was determined by the direct observation of nanorods with transmission electron microscopy. We estimated the growth rate of nanorods from the change in the average long-axis length over time. To understand the experimental results, we developed a mathematical model for the growth of nanorods. The present results should help to clarify the mechanism of the growth of gold nanorods.

Various kinds of nanostructures have been synthesized for use as new materials in nanotechnology and in industrial applications [1]. Among these, gold nanorods are some of the most interesting objects, and they typically range in length from several nanometers to over 1 μm [2–8]. Gold nanorods are often synthesized by using a surfactant solution, and previous reports have considered the mechanism of the growth of gold nanorods [9–13]. Johnson *et al.* [9] studied the mechanism from the viewpoint of the crystal structure at the surface of gold nanorods, and Gao *et al.* [10] focused on the van der Waals stabilization of the surfactant bilayer on the gold surface. Perez-Juste *et al.* [11] proposed an electrochemical mechanism where rod formation is controlled by the directional collisions of Au-bound micelles. Recently, Zhou and Huang [12] proposed a characteristic length scale on nanorod growth with the aid of lattice kinetic Monte Carlo simulation. Nishioka *et al.* [13] indicated that the photoreactions of ketones should trigger the nanorod formation in photochemical synthesis. However, the mechanism of the growth of gold nanorods has not yet been fully understood.

To better understand the dynamic process of growth, for example, the growth rate, it may be helpful to observe the change in the growth of gold nanorods over time. In some previous studies, the kinetics during the growth process has been observed by spectroscopy. A few metal nanostructures, including gold nanospheres, exhibit characteristic absorption bands in the visible part of the spectrum. This characteristic absorption is caused by the interaction of light with surface plasmon, and thus the absorbed wavelength depends on the size, shape, surface properties, and so on of the nanostructures [14–16]. Hence, spectroscopic measurements are usually used to monitor the average size and shape of an assembly of gold nanostructures obtained in high yield [7,8,11,17–22]. In fact, by studying the change in the spectrum over time, Jana *et al.* [7] reported that particle growth was faster in the presence of a large amount of seed particles. Sau and Murphy showed that an increase in the short-axis

length follows an increase in the long-axis length of nanorods (aspect ratio is less than 5). They also characterized nanorods by transmission electron microscopy (TEM) without stopping the chemical reactions [8]. Perez-Juste [11] showed visible spectra at different stages in the growth of nanorods to measure the growth rate.

When nanorods are obtained in high yield, it is useful to observe spectral changes over time, as shown above, and such measurements can be performed without stopping the chemical reactions during growth. However, when nanorods are obtained in low yield, it is difficult to determine information regarding the long-axis and short-axis lengths of nanorods from spectroscopic data because experimental spectral data include an averaging procedure over a wide range of sizes and shapes of nanostructures, and relevant features of spectra are smoothed out [23]. In this Rapid Communication, we establish an experimental method for completely stopping the growth of gold nanorods at any instant. This method enables us to observe the growth of nanorods in low yield. From the data we obtained with this method, we also present a model for reproducing the growth process of nanorods based on the information regarding the changes in the long-axis and short-axis lengths of nanorods over time, as directly obtained by TEM observation. Such a numerical simulation with experimental parameters makes it possible to estimate the growth rate of nanorods.

Before synthesis, 0.1 M hexadecyltrimethylammonium bromide (HTAB) (Tokyo Chemical Industry) solution was kept at 40 °C so that it would completely dissolve. For the synthesis of a seed suspension, 1875 μl of the surfactant solution (40 °C), 62.5 μl of 0.01 M tetrachloroaurate acid tetrahydrate (HAuCl$_4$·4H$_2$O, Nacalai) solution, and 150 μl of 0.01 M sodium borohydride (NaBH$_4$, Nacalai) solution were mixed at a temperature of 40 °C in this order. As soon as NaBH$_4$ was added, the solution was rapidly mixed for 2 min and the evolved gas was allowed to escape. The resulting brown suspension of gold seeds was stored at 40 °C for over 2 h. For the formation of nanorods, 9500 μl of the surfactant solution (40 °C), 400 μl of 0.01 M tetrachloroaurate acid tetrahydrate solution and 64 μl of 0.1 M ascorbic acid (C$_6$H$_8$O$_6$, Nacalai) solution were mixed at 40 °C in this order. With these procedures, the color of the solution van-

———————
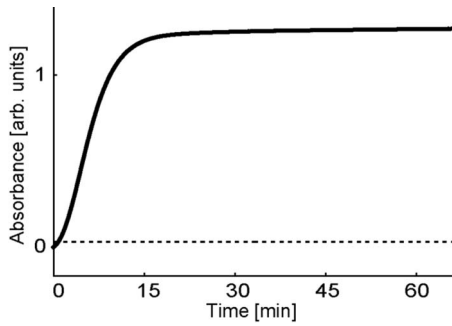*Corresponding author. FAX: +81-48-462-4695; ytakenaka@riken.jp

FIG. 1. Time changes in the adsorbed peak intensities at 550 nm just after adding seed. Without adding dodecanethiol-ethanol solution (thick line), the intensity increases gradually and saturates. With adding a dodecanethiol-ethanol solution (dotted line), the intensity is fixed. It means that the growth of nanoparticles completely stopped.

ished. Next, 17 μl of the prepared seed suspension was added and the solution was gently mixed for 10 s. The resulting colorless solution was stored at 20 °C and gradually became dense pink.

To observe the growth of nanorods over time, we stopped the chemical reactions at X minutes ($X=0.5, 1.0, 1.5, 2.0, 2.5, 3.0, 3.5, 4.0, 4.5, 5.0, 6.0, 8.0, 10, 15, 30, 60, 120, 180$) after we added the seed suspension, by adding 500 μl of 1% dodecanethiol-ethanol ($C_{12}H_{25}SH$, Wako Pure Chemical Industries) solution. The reaction-stopped suspension of gold nanorods was characterized by TEM (JEOL 1200EXII) after centrifugation. At centrifugation, 1400 μl of the resulting suspension was centrifuged at 5000 rpm for 5 min and the upper transparent part was removed. The lower part was redispersed in 700 μl of purified water and centrifuged again at 5000 rpm for 5 min. After the upper transparent part was removed, the precipitated dense suspension was used to prepare TEM samples by placing 15 μl of the suspension on a carbon-coated copper grid for 1 min. After the excess part was removed, it could be used for TEM observation.

Figure 1 shows the time changes in the adsorbed peak intensities at 550 nm of the growth suspensions during the growth. To observe the peak intensities makes it possible to confirm whether nanorods are growing or not because the peak intensity is approximately proportional to the total volume of nanoparticles. In case of the sample mixed with 500 μl of 1% dodecanethiol-ethanol solution 1 min after adding seed suspension, the growth stopped completely, while the intensity increases gradually for the sample without dodecanethiol-ethanol solution. The reaction-stopped suspensions were stable at least two weeks. Figures 2(a) and 2(b) show a time series of TEM images and the colors of the reaction-stopped suspensions of each sample, respectively. Figure 2(a) shows the average increases in the long-axis length. A TEM image taken 0.5 min after we added the seed suspension is not shown here since we could not find any visible object. As nanorods grow, the color of the suspension changes from transparent to dense pink because of the surface plasmon [Fig. 2(b)]. The changes in the average values of the long-axis length, short-axis length, and aspect ratio over time were measured by TEM observation and are

shown in Fig. 2(c) along with standard deviations. This indicates that rod growth was almost finished at 10 min after we added the seed suspension.

To discuss the growth process of nanorods, we present a numerical model to calculate the average values (with standard deviations) of the size of nanorods. In this model, we make the following five assumptions: (A1) All objects grow to nanorods and all of the Au ions are used for nanorods. (A2) Nanorods are cylindrical. (A3) Every nanorod grows from a seed particle; i.e., there is no spontaneous nucleation. (A4) The growth rates of the long-axis and short-axis lengths are proportional to the reaction rate coefficients and the concentration of Au ions. (A5) The reaction rate coefficient is constant for the growth of the long-axis length but is a decreasing function of the concentration of Au ion for the short-axis length. This is because the current understanding of the anisotropic shape is induced by the preferential adsorption of the surfactants to high-energy facets of rods [24].

By considering the reaction kinetics based on the above-mentioned assumptions, we derived evolutional equations for the concentration of Au ions, c, and the distribution of the number density of gold nanorods, $n(L,D)$, with a long-axis length of L and a short-axis length of D. For simplicity, we considered that the long-axis length L and short-axis length D have discrete values, i.e., $L = i\Delta L$ and $D = j\Delta D$, where i and j are integers. Here we consider the evolutional equation for $n(L,D)$. According to assumption (A4), the time derivative of number of nanorods $n(L,D)$ whose long-axis length is L and short-axis length D is expressed as the following equation:

$$\frac{d}{dt}n(L,D) = K_1 cn(L - \Delta L, D) + K_2(c)cn(L, D - \Delta D)$$
$$- [K_1 + K_2(c)]cn(L,D). \tag{1}$$

Here, $K_1 cn(L-\Delta L, D)$, $K_2(c)cn(L, D-\Delta D)$, and $[K_1 + K_2(c)]cn(L,D)$ are the number of nanorods whose long-axis length grow from $L-\Delta L$ to L, that whose short-axis length grow from $D-\Delta D$ to D and that whose long-axis or short-axis length grow from L or D to $L+\Delta L$ or $D+\Delta D$, respectively. Here, K_1 and $K_2(c)$ are the reaction coefficients for the growth of the long-axis length and that for the short-axis length, respectively.

Next, we consider the evolutional equation for c. According to the assumption (A1), since the decrease in the concentration of Au ion should be proportional to the summation of the increasing volume of nanorods, the following equation holds:

$$\frac{d}{dt}c = -\alpha \sum_L \sum_D \{K_1 cn(L,D)[V(L + \Delta L, D) - V(L,D)]$$
$$+ K_2(c)cn(L,D)[V(L, D + \Delta D) - V(L,D)]\}, \tag{2}$$

where $V(L,D)$ is the volume of a cylinder with a long-axis length of L and a short-axis length of D, i.e., $V = \pi L D^2 / 4$. Therefore, we can achieve the evolutional equation for c:
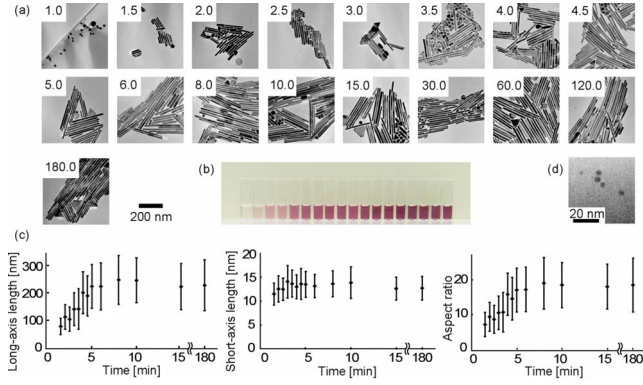
FIG. 2. (Color online) Experimental observations for the time series of reaction-stopped suspensions. (a) TEM images of the time series of the growth process of gold nanorods. The numbers in each image indicate the time interval (min) when the chemical reactions for nanorod growth were stopped by addition of the dodecanethiol-ethanol solution. (b) Images of the time series of reaction-stopped suspensions. (c) Time series of the average long-axis length, short-axis length, and aspect ratio of gold nanorods with standard deviations measured from the TEM images shown in (a). (d) TEM image of seed particles. The typical diameter is 5 nm.

$$\frac{d}{dt}c = -\alpha c \sum_L \sum_D \left[K_1 \frac{\pi D^2}{4}\Delta L + K_2(c)\frac{\pi DL}{2}\Delta D \right] n(L,D),$$

(3)

where α is the constant. Based on assumption (A5), we assume the reaction rate coefficient $K_2(c)$:

$$K_2(c) = \frac{K_{20}}{2}\left[\tanh\left(\frac{c-\bar{c}}{\kappa}\right) + 1 \right].$$

(4)

This is one of the simplest forms to express that the growth of short axis almost stops when the concentration of Au ion, c, is less than $\bar{c}$.

The initial condition for $n(L,D)$ is given as the Gaussian distribution with a cut-off:

$$n(L,D) = \begin{cases} N_0 \exp\left(-\frac{(L-L_{\mathrm{ini}})^2 + (D-D_{\mathrm{ini}})^2}{w}\right)/Z \\ \quad \text{if } |L-L_{\mathrm{ini}}| \le L_R \text{ and } |D-D_{\mathrm{ini}}| \le D_R \\ 0, \quad \text{otherwise}, \end{cases}$$

(5)

where

$$Z = \sum_{L=L_{\mathrm{ini}}-L_R}^{L_{\mathrm{ini}}+L_R} \sum_{D=D_{\mathrm{ini}}-D_R}^{D_{\mathrm{ini}}+D_R} \exp\left(-\frac{(L-L_{\mathrm{ini}})^2 + (D-D_{\mathrm{ini}})^2}{w}\right)$$

and N_0 corresponds to the initial number of seed particles.

Then, we discuss on the parameters considering the experimental condition. For the numerical simulation, we set the spatial unit $\alpha\Delta L$ and $\alpha\Delta D$ to be 1, where $\alpha = 2$ nm^{-1} and $\Delta L = \Delta D = 0.5$ nm. Based on an additional observation by TEM (JEOL JEM-2000FX), the representative size of seed particles is about 5 nm, as shown in Fig. 2(d) corresponding to the size reported by Keul *et al.* [24]. Thus, we regarded a
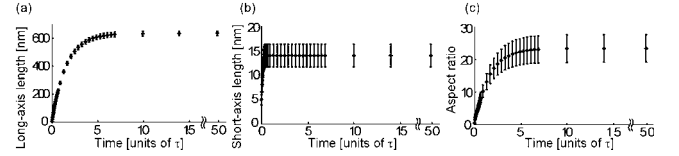

FIG. 3. Numerical results. Changes in the (a) long-axis length, L, (b) short-axis length, D, and (c) aspect ratio over time.

seed particle as a cylinder with a short-axis length and long-axis length of 5 nm, i.e., $D_{\mathrm{ini}} = 5$ nm and $L_{\mathrm{ini}} = 5$ nm.

Next, we consider the initial condition for c and n by regarding a cube with an edge of 0.5 nm as a volume unit. The concentration of Au ion is also considered based on the number of Au atoms including in this volume unit: a cube with an edge of 0.5 nm contains $0.5^3/0.3^3 \sim 5$ atoms since the characteristic distance between Au atoms in a crystal is about 0.3 nm. The initial number of seed particles that are included in 17 μl of seed suspension is calculated to be 6.1×10^{11} from the characteristic size of the seed. On the other hand, the growth solution contains about 2.4×10^{18} Au ions. Thus, the number of Au atoms per one seed in the growth solution can be calculated as 3.9×10^6, which corresponds to 8.0×10^5 volume units. In numerical calculation, we set N_0 equals unity, i.e., the total number of seeds is set as unity. In such a case, $c_0 = 8.0 \times 10^5$ from the above discussion. It is noted that the concentration and the scale of length are calculated directly from the experiments. Thus, the spatial scale can be considered quantitatively.

On the other hand, we cannot theoretically determine K_1, K_{20}, and $\bar{c}$, which relate with the rate coefficient. In the present Rapid Communication, we choose the following parameter so that the numerical results have good correspondence with the experimental ones: $K_1 = 0.001/\tau$, $K_{20} = 0.0001/\tau$, and $\bar{c} = 700\,000$, where τ is a time unit.

L_R, D_R, and w are the parameters for the initial distribution of the seed size and κ is the parameter that relates with the reaction rate of a short axis. These parameters do not play an important role to determine the growth process (data not shown). Here we set $\kappa = 0.5$, $D_R = 2.5$ (nm), $L_R = 2.5$ (nm), and $w = 1$ (nm^2).

We made a numerical calculation based on Eqs. (1) and (3)–(5) using the Euler method with a time step of $\Delta t = 10^{-4}$. The changes in the average long-axis length, short-axis length, and aspect ratio over time with the above-mentioned parameters by the numerical simulation are shown in Fig. 3. In these parameters, the numerical results represent the experimental results quantitatively on the spatial scale. If the time unit τ corresponds to 2 min, the time scale is also represented as shown in Figs. 2 and 3. Thus, from the parameters, we can guess that gold nanorods grow in the long-axis direction about 1.3×10^5 atoms/s/nm^2 at the initial stage. In contrast, from a kinetic theory of a dilute solution, we can suppose that 6.2×10^7 atoms s/nm^2 collide against a gold nanorod in the growth solution under the present experimental conditions. Thus, about one of 100 Au atoms that collide with a nanorod contributes to nanorod growth if we assume that an Au atom exists as a single element. However, since it has been reported that an Au atom forms a complex with a surfactant micelle composed of
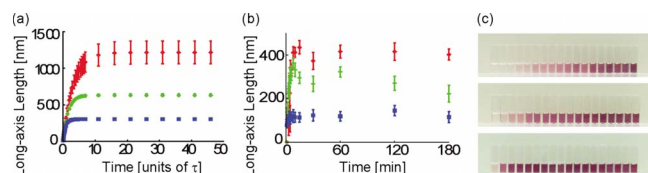
FIG. 4. (Color online) Dependence of the change in the long-axis length with time on the amount of seed particles. (a) Numerical results with changes in the parameter N_0. N_0 is 0.2 (top; red), 1 (middle; green), and 5 (bottom; blue). (b) Experimental results with various amounts of seed particles. 3.4 (top; red), 17 (middle; green), and 85 (bottom; blue) μl of seed suspension were added to the growth solution, respectively. (c) Images of the time series of reaction-stopped suspensions corresponding to the experimental results in (b). 3.4 (top), 17 (middle), and 85 (bottom) μl of seed suspension were added to the growth solution, respectively.

around 100 molecules [11], about one of 10 Au-micelle complexes that collides with a nanorod might contribute to its growth.

From the above correspondence between our experimental and numerical results, our five assumptions [(A1)–(A5)] are considered to be appropriate. Any quantitative disagreement should be due to spontaneous nucleation and the yield; not all of the products are rods, and the experiments include a few spheres and polyhedrons.

As demonstrated in the above estimation, the number of seed particles added to the growth solution strongly affects the long-axis length of gold nanorods. To confirm the adequacy of the numerical model, we changed the parameter N_0, which corresponds to the initial number of seed particles in the growth solution both theoretically and experimentally. In Fig. 4(a), the numerical results show the following: (B1) the average long-axis length of nanorods is longer if the initial number of seed particles is less; (B2) the time for the saturation of the long-axis length of nanorods is longer if the initial number of seed particles is less; and (B3) the initial

growth rates of the long-axis length are the same even if we change the initial number of seed particles, and this is also true for the initial growth rate of the short-axis length. Along with the numerical model, we performed experiments by changing the number of seed particles. With different amounts of seed suspension, we synthesized nanorods by the same method as described in the experimental section and observed the changes in the average long-axis length of nanorods over time [Fig. 4(b)]. As shown in Figs. 4(a) and 4(b), the experimental results qualitatively correspond to the numerical predictions (B1), (B2), and (B3). Figure 4(c) also indicates, from the viewpoint of the absorption of surface plasmon, that as fewer seeds are included, an increasingly greater time is needed for saturation to the resulting long-axis length (B2).

In summary, by using dodecanethiol–ethanol solution, the growth process of gold nanorods could be stopped experimentally and the time series of the average values of the long-axis length, short-axis length, and aspect ratio were measured. To understand the experimental results, a model for the growth of gold nanorods was presented. We were able to estimate the growth rate of nanorods by performing a numerical calculation with a model with the experimental parameters. For the better understanding of the growth mechanism of gold nanorods, to determine K_1 and $K_{2(c)}$ quantitatively will be helpful by considering the effect of Ag(I) in regulating the growth rate along the various crystallographic planes. It is also helpful to consider the reconstruction process at side facets of nanorods [24].

[1] Y. Xia *et al.*, Angew. Chem., Int. Ed. **48**, 60 (2009).

[2] Y. Takenaka and H. Kitahata, Chem. Phys. Lett. **467**, 327 (2009).

[3] M. T. Reetz and W. Helbig, J. Am. Chem. Soc. **116**, 7401 (1994).

[4] Y.-Y. Yu *et al.*, J. Phys. Chem. B **101**, 6661 (1997).

[5] K. Esumi *et al.*, Langmuir **11**, 3285 (1995).

[6] F. Kim *et al.*, J. Am. Chem. Soc. **124**, 14316 (2002).

[7] N. R. Jana *et al.*, J. Phys. Chem. B **105**, 4065 (2001).

[8] T. K. Sau and C. J. Murphy, Langmuir **20**, 6414 (2004).

[9] C. J. Johnson *et al.*, J. Mater. Chem. **12**, 1765 (2002).

[10] J. Gao *et al.*, Langmuir **19**, 9065 (2003).

[11] J. Perez-Juste *et al.*, Adv. Funct. Mater. **14**, 571 (2004).

[12] L. G. Zhou and H. Huang, Phys. Rev. Lett. **101**, 266102 (2008).

[13] K. Nishioka *et al.*, Langmuir **23**, 10353 (2007).

[14] J. Pérez-Juste *et al.*, Coord. Chem. Rev. **249**, 1870 (2005).

[15] M. Pelton *et al.*, Phys. Rev. B **73**, 155419 (2006).

[16] K. Imura and H. Okamoto, Phys. Rev. B **77**, 041401(R) (2008).

[17] K. Torigoe and K. Esumi, Langmuir **8**, 59 (1992).

[18] B. Nikoobakht and M. A. El-Sayed, Chem. Mater. **15**, 1957 (2003).

[19] G. Carotenuto and L. Nicolais, J. Mater. Chem. **13**, 1038 (2003).

[20] J. Boleininger *et al.*, Phys. Chem. Chem. Phys. **8**, 3824 (2006).

[21] T. H. Ha *et al.*, J. Phys. Chem. C **111**, 1123 (2007).

[22] X. Kou *et al.*, Chem.-Eur. J. **13**, 2929 (2007).

[23] I. O. Sosa *et al.*, J. Phys. Chem. B **107**, 6269 (2003).

[24] H. A. Keul *et al.*, Langmuir **23**, 10307 (2007).